Soldagem & Inspeção

Influence of Pin Shape Geometry on the Torque, Forces, and Residual Stresses in Friction Stir Welding of 5052-H34 Aluminum Alloy

Karen Johanna Quintana[1] , Maria Cindra Fonseca[2] , Jose Luis Silveira[3]

[1] Universidade Federal do Rio de Janeiro, Instituto Alberto Luiz Coimbra de Pós-graduação e Pesquisa de Engenharia – COPPE, Departamento de Engenharia Mecânica, Rio de Janeiro, RJ, Brasil.

[2] Universidade Federal Fluminense, Departamento de Engenharia Mecânica, Programa de Pós-graduação em Engenharia Mecânica – PGMEC, Niterói, RJ, Brasil.

[3] Universidade Federal do Rio de Janeiro, Instituto Alberto Luiz Coimbra de Pós-graduação e Pesquisa de Engenharia – COPPE, Escola Politécnica, Departamento de Engenharia Mecânica, Rio de Janeiro, RJ, Brasil.

Abstract: The torque and forces in friction stir welding (FSW) are important parameters for the process behavior, weld quality, and mechanical properties of the weld. Torque and forces are mainly influenced by rotational and welding speeds and tool geometry, including the tool pin profile. However, experimental studies to describe the influence of the pin profile on torque and forces have received little attention. In this paper, the influence of the threaded pin on torque and forces in the FSW process of 5052-H34 aluminum alloy is considered. The axial, welding, and transverse forces and the torque are experimentally measured at several combinations of rotational (600, 900, 1200 and 1500 rpm) and welding speeds (100, 200, and 300 mm/min) for two pin profiles: smooth and threaded. Additionally, residual stresses are measured, by X-ray diffraction technique, for some experimental conditions in the stir zone of the weld. The results show that the influence of the pin shape on the torque, forces, and residual stresses depends on the rotational and welding speeds, mainly on the rotational speeds. In general, the threaded pin increases the residual stresses and the maximum values of torque and forces in the axial and transverse directions while reducing the welding force.

Keywords: Friction stir welding; 5052-H34 aluminum alloy; Experimental torque and forces; Residual stresses; Pin shape.

1. Introduction

Friction stir welding (FSW) is a solid state welding technique that has been widely studied in the last years to weld aluminum and magnesium alloys [1], titanium alloys [2], polymers and polymer matrix composites [3], aluminum matrix composites [4], stainless steel [5,6], Inconel [7], dissimilar materials [8] among others. Owing to the absence of melting in the welding, less energy is required to produce high quality welds, thence the process is cost-efficient and environmentally friendly [9].

In the FSW process, there is a system composed by three forces, the axial, welding, and transverse forces, and the torque acting on the tool. The forces and the torque influence the tool design, the selection of the machine, and the weld quality. Comparing the three forces, the axial force is the higher force of the process. Its maximum value is presented during the plunging phase, at the beginning of the process, when the material around the tool is not softened and offer more resistance to penetration due to a higher local yield stress. Therefore, the axial force is important for the proper selection of the welding machine [10]. During the welding phase, the tool is submitted to a compressive stress by the action of the axial force and shear stresses by the action of the welding and transverse forces. However, the magnitude of the welding force is significantly higher than the transverse force [11].

The analysis of the welding and transverse forces is an important aspect to avoid tool breakage during the welding phase. Additionally, the transverse force can be an indicator of the asymmetry of the weld [12]. Dialami et al. [12] attributed the presence of the transverse force to a lack of symmetry of the weld, due to an asymmetric contact at the front and back sides of the tool. This produces higher temperatures at the front side of tool. Consequently, lower local yield stress of the material causing a force in the $\omega \times v_w$ direction (where ω is the rotational speed and v_w the welding speed). Moreover, Quintana and Silveira [13] computed the power in FSW from torque measurements and, according to Cui et al. [14], the torque is strongly related to the power consumption during the process. For this reason, the torque

Influence of Pin Shape Geometry on the Torque, Forces, and Residual Stresses in
Friction Stir Welding of 5052-H34 Aluminum Alloy

Quintana et al.

knowledge is important for the selection of the motor capacity of FSW machines [10]. The axial force in FSW is related to the quality of the welds [15]; therefore, the control of the axial force during the FSW process is important to produce defect free welds. According to Zhao et al. [16], clamping, tool, and machine failures during the process can be reflected in the axial force signal. Shrivastava et al. [9] measured the forces in the FSW of aluminum alloy AA6061-T6 and correlated some signal parameters of the forces to the appearance and size of discontinuities during FSW.

The forces and torque in FSW are influenced by the tool geometry and the material properties [17] and by the rotational and welding speeds [18]. The temperature in the process is related to the tool geometry by means of the contact area at tool-material interface. The contact area affects the friction during the welding process and, consequently, the temperature [10]. According to Mishra and Ma [19] the temperature in the FSW process is mainly generated by the friction at the tool-material interface and by the plastic deformation of the material.

The mixing of the material during the FSW process depends on the pin geometry. Therefore, it influences the temperature, material flow and forces of the process and, consequently, it affects the quality of the joint [12]. Rao et al. [20] compared experimentally five types of pin geometries. The authors found that the tool pin profile influences the weld nugget microstructure, hardness, and corrosion properties. This can be related to the heat input and material flow produced by the specific pin profile.

FSW process can be interpreted as a combination between forging and extrusion with high deformation rates [21]; therefore, FSW produces a residual stress field, as any manufacture process, due to the thermal cycles and the plastic deformation. The residual stresses induced in the welding process can affect the mechanical performance of the weld [22]. Although the tensile residual stresses can reduce the strength of the mechanical components inducing brittle fractures [23], the compressive residual stress present a beneficial effect, as they avoid the nucleation and propagation of fatigue cracks [24]. Aval [25] found that the increase of the heat input increases the residual tensile stress region in FSW. Moreover, Zapata et al. [26] observed that the rotational speed has a significant influence on the residual stresses behavior in FSW; consequently, the evaluation of the residual stress in FSW is important and necessary for a proper design of the welded joint.

Despite the importance of the forces, torque, and residual stresses for the process efficiency and quality of the weld, few studies have been developed with this focus [9,15,20]. Therefore, this paper describes the influence of the threaded pin on the residual stresses, on the torque and forces of the process. FSW experiments are performed for two combinations of tool pin profile (smooth and threaded) and several welding and rotational speeds. The residual stresses are measured in the stir zone of the weld produced by both pin shapes and some conditions of the rotational and welding speeds. The results show that all the evaluated variables are influenced by the interaction between the effects of the pin shape, the rotational and the welding speeds.

2. Experimental Procedure

Aluminum alloy 5052-H34 plates with dimensions 60 x 35 x 5 mm (a thickness of 5 mm, a width of 60 mm and a length of 35 mm) were welded by the FSW technique. The chemical composition and the mechanical properties of the aluminum alloy provided by the supplier are presented in Table 1. The welding was conducted in a computer numerical control (CNC) machine adapted to the process. A Kistler 9272 dynamometer and a Kistler 5070 multichannel charge amplifier were used to measure the torque and forces and for the signal conditioning of the data, respectively. The dynamometer is able to measure the forces in three orthogonal axes in any position and the torque in its center; therefore, two groups of experiments were presented. A group to measure the torque during the plunging phase and another one to measure the torque in the welding phase, in which, the torque presents a steady state regime as observed by Kumar et al. [27].

Table 1. Chemical composition and mechanical properties of 5052-H34 aluminum alloy.

Chemical composition (% weight)							
Al	Fe	Mn	Si	Cr	Cu	Mg	Zn
95.7-97.7	0.4 max.	0.1 max.	0.25 max.	0.15-0.35	0.1 max.	2.2-2.28	0.1 max.
Mechanical properties							
Tensile strength (MPa)		Yield strength (MPa)		Elongation (%)		Hardness (HV)	
262		214		10		78	

The experiments were conducted at several levels of rotational and welding speeds, and pin shape factors. The experimental design is presented in Table 2 and the tools used to carry out the experiments are shown in Figure 1. The experimental data for smooth pin were taken from: Quintana and Silveira [28] for the torque and Quintana and Silveira [11] for the forces.

Influence of Pin Shape Geometry on the Torque, Forces, and Residual Stresses in
Friction Stir Welding of 5052-H34 Aluminum Alloy

Quintana et al.

Table 2. Experimental design to conduct the experiments.

| Welding parameter	Value
Rotational speed (ω)	600, 900, 1200 and 1500 rpm
Welding speed (v_w)	100, 200, and 300 mm/min
Plunging speed	8 mm/min
Pin shape (P_s)	Threaded (M4 standard thread) and Smooth
Shoulder diameter	10 mm
Pin diameter	4 mm
Pin length	4 mm
Total plunging depth	4.2 mm
Tool material	H13 steel heat treated for 50 HRC
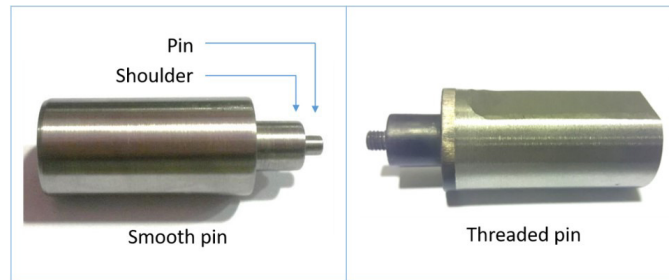
Figure 1. Threaded and smooth pin tools used to conduct experiments.

To evaluate the influence of the tool pin profile on the residual stresses, the limit conditions for the rotational and welding speeds were selected. The residual stresses measurements were conducted for the joints performed at rotational speeds of 600 and 1500 rpm and welding speeds of 100 and 300 mm/min, using two types of pin profile: a threaded and a smooth pin. Surface residual stresses were analyzed by X-ray diffraction technique using $\sin^2\psi$ method [29] for which the lattice spacing d of material was measured at five inclination angles. Measurements were carried out with a Stresstech Xstress3000 portable analyzer with a 1.0-mm diameter collimator (30 kV and 6.7 mA) and its values calculated by XTronic V1-0 Standard software. Measurement parameters are depicted in Table 3. Residual stress measurements were performed in the stir zone of the weld in the longitudinal (L) and transversal (T) directions in relation to the welding direction, as shown in Figure 2.

Table 3. Parameters used for the X-ray residual stress analysis.

Parameter	Value
Diffraction plane of Al (hkl)	(222)
Radiation	CrKα
Wavelength (λ)	2.29092 Å
Bragg angle 2θ (º)	156.98°
Inclination angles ψ	0, 18, 27, 33 and 45°
Exposure time (s)	50
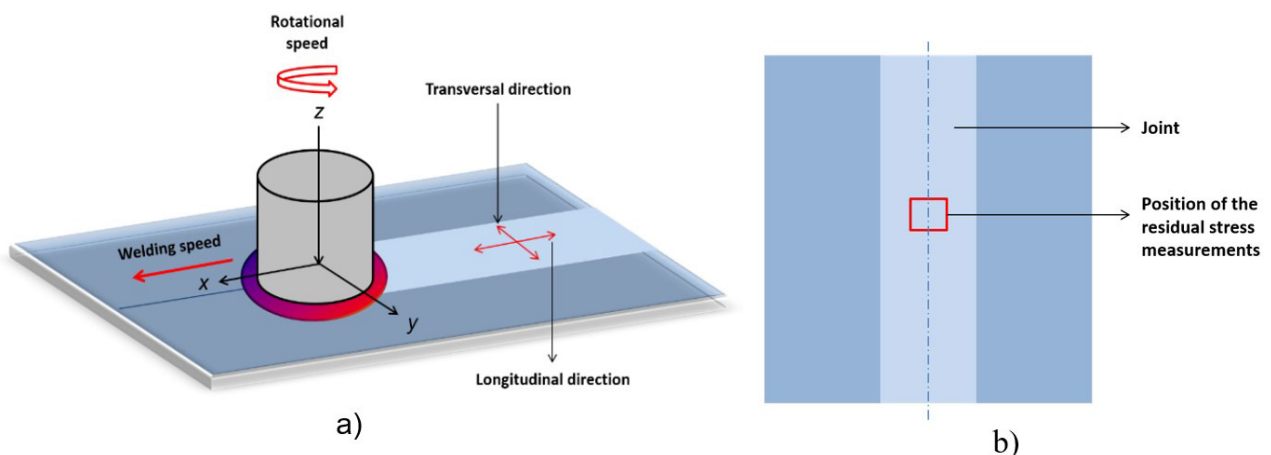
Figure 2. (a) Measurement directions and (b) schematic position of the residual stresses measurements in FSW joint

Influence of Pin Shape Geometry on the Torque, Forces, and Residual Stresses in
Friction Stir Welding of 5052-H34 Aluminum Alloy

Quintana et al.

3. Results and Discussion

3.1. Torque during FSW

Figure 3a shows the torque with the variation of time during the plunging phase of the FSW process for the rotational speeds of 600 rpm and 1500 rpm, respectively. The torque achieves the maximum value when the shoulder makes contact with the material and the plunging phase finishes with the total plunging depth of the tool (4.2 mm). In the plunging phase, the smooth pin presents higher or similar torque values during most part of the plunging phase. In the end of this phase, due to the effect of the shoulder, the maximum torque value of the threaded pin exceeds the maximum torque value of the smooth pin. The threaded pin improves the flow of the material around the tool; therefore, the torque required to stir the material diminishes. Jain et al. [30] predicted higher strain rate, material velocity, and vertical flow for a threaded conical pin when compared to a smooth conical pin. For lower rotational speeds, the effect of the thread is more significant on the torque value. While for higher rotational speeds, the effect of the thread on the torque is considerably reduced because of the higher heat input. In the welding phase, the torque is smaller than the maximum torque value presented in the plunging phase owing to the heat softening of the material.
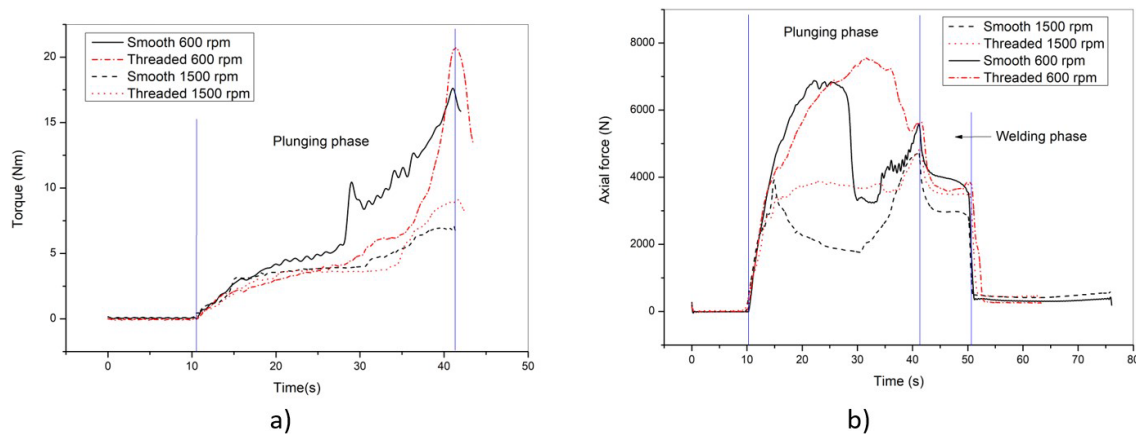

a)   b)

Figure 3. (a) Torque and (b) Axial force with the variation of time at 600 and 1500 rpm.

Figure 4 shows the maximum torque in the plunging phase and the steady state torque value in the welding phase, as a function of the rotational speed. In general, the torque diminishes with higher rotational speeds due to the increase of the heat input into the process. This decreases the local yield stress of the material and, consequently, the torque decreases. As observed in Figure 4a, in the plunging phase, the maximum torque value is higher for the tool with the threaded pin. The welding speed does not present influence on the maximum torque value. In the welding phase (Figure 4b), for low rotational speeds, the torque for the smooth pin presents higher values than the torque for the threaded pin. On the contrary, for high rotational speeds the torque for the smooth pin presents the same or smaller values than the torque for the threaded pin. This behavior can indicate that, as observed in Figure 3a, the effect of the threaded pin on the material is reduced with the increase of the heat input into the process. Table 4 presents the analysis of variance (ANOVA) for the maximum torque (M) during the plunging phase and the stabilized torque (S) in the welding phase. In the plunging phase, only the rotational speed and the pin shape factors have influence on the maximum torque. The maximum torque is affected by the interaction of these factors. In the welding phase, there is an interaction between the effects of the three evaluated factors (pin shape, rotational and welding speeds) on the stabilized torque. In both phases, the torque is mainly influenced by the rotational speed.
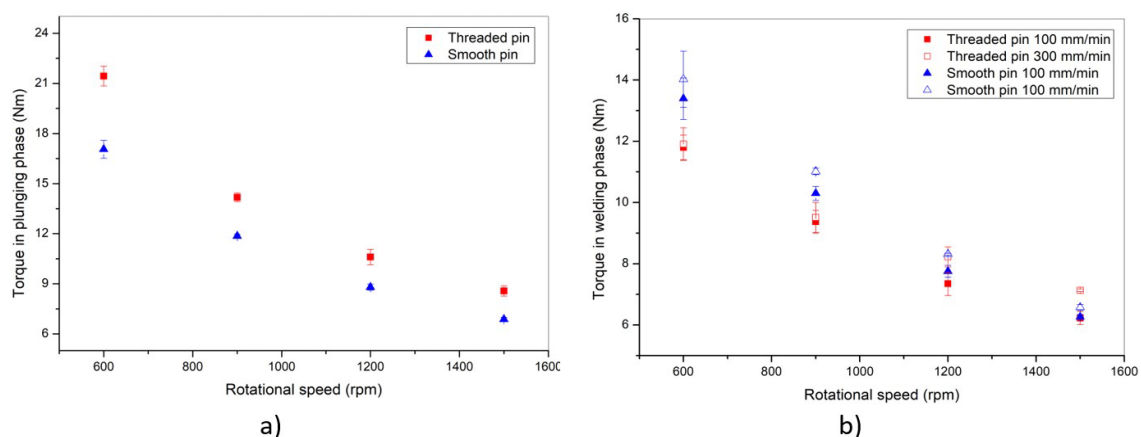

a)   b)

Figure 4. Torque variation with the rotational speed for (a) the plunging phase and (b) the welding phase.

Influence of Pin Shape Geometry on the Torque, Forces, and Residual Stresses in
Friction Stir Welding of 5052-H34 Aluminum Alloy

Quintana et al.

Table 4. ANOVA for the maximum torque (M) in plunging phase and the stabilized torque (S) in welding phase.

Source	Sum square		Dof	Mean square		F		p-level	
	M	S	M-S	M	S	M	S	M	S
ω	1374.63	421.782	3	458.21	140.594	2020.19	764.6	0	0
v_w	0.48	3.463	2	0.241	1.732	1.06	9.42	0.3536	0.0004
P_s	116.94	6.189	1	116.94	6.189	515.58	33.66	0	0
$\omega * v_w$	2.03	2.207	6	0.338	0.368	1.49	2	0.2024	0.0839
$\omega * P_s$	21.11	16.614	3	7.038	5.538	31.03	30.12	0	0
$v_w * P_s$	0.08	1.165	2	0.042	0.582	0.18	3.17	0.8326	0.051
$\omega * v_w * P_s$	0.99	2.956	6	0.166	0.493	0.73	2.68	0.6272	0.0252
Error	10.89	8.826	48	0.227	0.184				
Total	1527.15	463.203	71						

3.2. Axial force during the FSW

Figure 3b shows the axial force behavior as a function of time for the welds performed with both pin shapes (smooth and threaded), a welding speed of 100 mm/min, and rotational speeds of 600 rpm and 1500 rpm. For the rotational speed of 600 rpm the maximum axial force is higher for the threaded pin. This behavior can be related to the increase of the contact area at the tool-material interface caused by the thread of the pin. At the end of the plunging phase the axial force presents the same value for both pin shapes by the shoulder effect. During the welding phase, the axial force for smooth pin present higher values and at the end of the experiment the axial force for the threaded pin increases slightly. For 1500 rpm, the maximum axial force at the end of the plunging phase present similar values for both pin shapes due to the effect of the shoulder. During the welding phase, the axial force is stabilized and is higher for the threaded pin until the end of the experiment. The effect of the threaded pin on the material flow can be less relevant for higher rotational speeds. This is due to the increase in the heat input, and under this condition, the increment of the contact area by the thread of the pin is probably more relevant.

Figure 5 presents the axial force as a function of the rotational speed for the plunging and welding phases. Figure 5a shows the maximum axial force of the plunging phase as a function of the rotational speed for both pin shapes: threaded and smooth. In all cases, the axial force for the threaded pin is higher; however, for higher rotational speeds the differences between the maximum axial force for threaded and smooth pins are reduced. The welding speed does not present influence on the maximum axial force, which happens during the plunging phase. During the welding phase, as observed in Figure 5b, the axial force is higher for the threaded pin from 900 rpm. In general, the axial force for the threaded pin presents a smaller influence by the rotation. This behavior of the axial force was observed for all the welding speeds. Table 5 presents the ANOVA for the maximum axial force (M) in the plunging phases and the stabilized axial force (S) in the welding phase. In the plunging phase, the axial force is mainly influenced by the rotational speed followed by the pin shape. The maximum axial force is influenced by the interaction of the rotational speed and pin shape factors. In the welding phase, the stabilized axial force is firstly influenced by the welding speed, secondly by the rotational speed, and finally by the pin shape. The analysis indicates that the stabilized axial force is influenced by the interaction of these three factors.

a)   b)
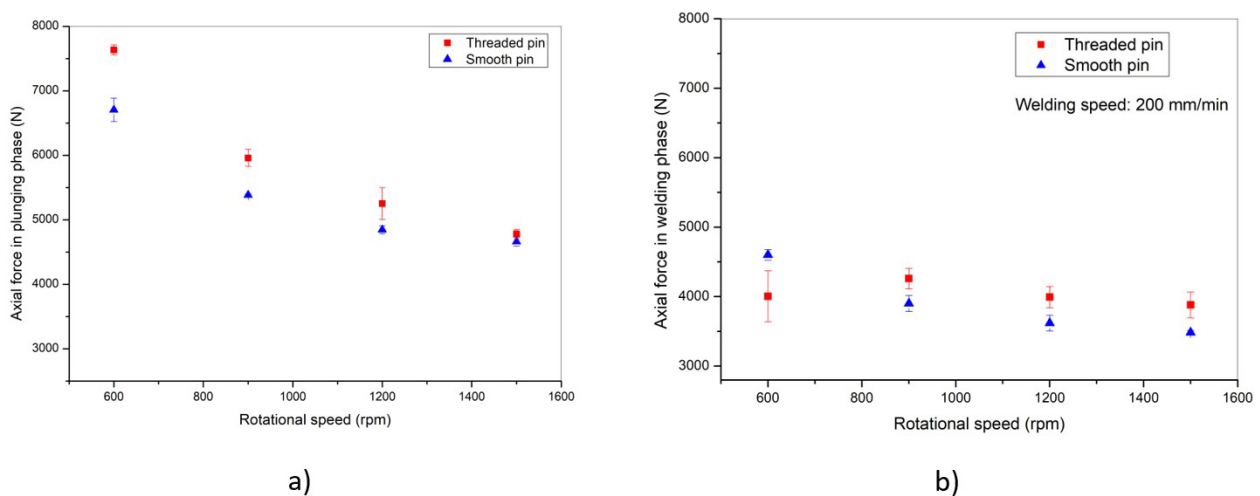
**Figure 5.** Axial force as a function of rotational speed for: (a) plunging phase; (b) welding phase at 200 mm/min.

Influence of Pin Shape Geometry on the Torque, Forces, and Residual Stresses in
Friction Stir Welding of 5052-H34 Aluminum Alloy

Quintana et al.

Table 5. Analysis of variance (ANOVA) for the axial force in the plunging (M) and welding (S) phases.

Source	Sum square		Dof	Mean square		F		*p*-level	
	M	S	M-S	M	S	M	S	M	S
ω	57973904.2	4678296.5	3	19324634.7	1559432.2	609.69	53.06	0	0
v_w	5005.7	6058585	2	2502.9	3029292.5	0.08	103.07	0.9242	0
P_s	5411707.3	692456.4	1	5411707.3	692456.4	170.74	23.56	0	0
$\omega * v_w$	180099.1	231686.5	6	30016.5	38614.4	0.95	1.31	0.4708	0.2693
$\omega * P_s$	590225.6	3091256.1	3	196741.9	1030418.7	6.21	35.06	0.0012	0
$v_w * P_s$	40076	134978.2	2	20038	67489.1	0.63	2.3	0.5358	0.1116
$\omega * v_w * P_s$	209327.8	734356.3	6	34888	122392.7	1.1	4.16	0.3758	0.0019
Error	1521401.7	1410776.9	48	31695.9	29391.2				
Total	65931747.4	17032392	71						

3.3. Welding and transverse forces during the FSW

Figure 6 shows the welding and transverse forces as a function of the rotational speed for a welding speed of 100 and 300 mm/min and both pin shapes. The welding force is higher than the transverse force and both forces are mainly influenced by the welding speed. Higher welding speeds diminish the available time to the heat input, consequently, the material is less softened and the force required to produce the weld increases. For all the welding speeds, the welding force is higher for the smooth pin than the threaded pin from 900 rpm, with exception of 300 mm/min that the force presents the same value for both pin shapes at 900 rpm. According to Jain et al. [30], the thread of the pin promotes the vertical flow of the material. This effect can reduce the resistance of the material to the advance of the tool. The vertical flow of the material affects the material that is in contact with the lateral area of the tool, which is directly related to the welding force and; therefore, the welding force is reduced. On the other hand, the transverse force is higher for the threaded pin in all cases with exception of the value for 600 rpm at 300 mm/min, which is equal for both pin shapes. These transverse force values can indicate that the asymmetry of the welds performed with a threaded pin is higher. Dialami et al. [12] studied, by simulation, the influence of the tool pin geometry on material flow, torque, and forces. The authors found that the lack of symmetry produced by different pin geometries is related to the transversal force.

Table 6 presents the ANOVA for the welding (W) and transverse (T) forces. The analysis indicates that, there are interactions between the effects of the pin shape, rotational and welding speeds on the welding and transverse force. Moreover, both forces are mainly influenced by the welding speed, followed by the pin shape, and finally by the rotational speed.
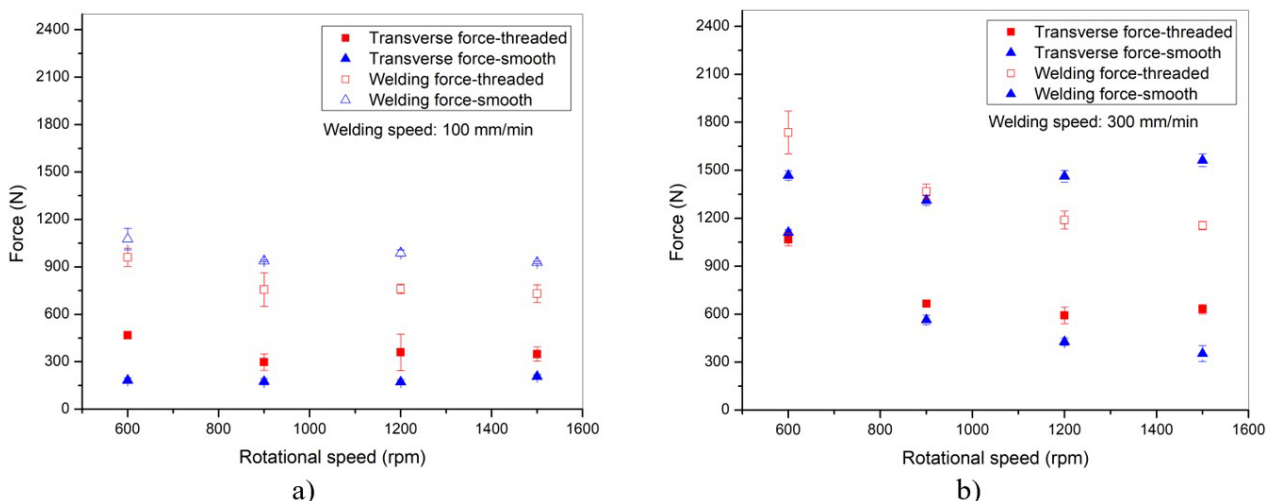
Figure 6. Welding and transverse forces as a function of the rotational speed for the threaded and smooth pins and the welding speeds of (a) 100 mm/min and (b) 300 mm/min.

Influence of Pin Shape Geometry on the Torque, Forces, and Residual Stresses in
Friction Stir Welding of 5052-H34 Aluminum Alloy

Quintana et al.

Table 6. Analysis of variance (ANOVA) for the welding (W) and transverse (T) forces.

Source	Sum square		Dof	Mean square		F		p-level	
	W	T	W-T	W	T	W	T	W	T
ω	629881.9	1004118.8	3	209960.6	334706.3	42.83	149.04	0	0
v_w	3172612.4	1932585	2	1586306.2	966292.5	323.62	430.29	0	0
P_s	581612	467431.5	1	581612	467431.5	118.66	208.15	0	0
$\omega * v_w$	48891.4	613203.2	6	8148.6	102200.5	1.66	45.51	0.1508	0
$\omega * P_s$	484132.5	8221.4	3	161377.5	2740.5	32.92	1.22	0	0.3125
$v_w * P_s$	98207.8	12050.5	2	49103.9	6025.3	10.02	2.68	0.0002	0.0786
$\omega * v_w * P_s$	193685.1	127152.8	6	32280.8	21192.1	6.59	9.44	0	0
Error	235280.8	107792.9	48	4901.7	2245.7				
Total	5444303.9	4272556.2	71						

3.4. Residual stresses in FSW

Figure 7 presents the residual stresses for the smooth and threaded pins, only for the limit conditions: 600 and 1500 rpm for the rotational speeds and 100 and 300 mm/min for the welding speeds. The results show that, for the smooth pin in the longitudinal direction, the residual stresses are fully compressive and are influenced by the rotational and welding speeds. For the welds obtained from a smooth pin, the conditions of 1500 rpm with 100 mm/min and 600 rpm with 300 mm/min presented residual stresses totally compressive in both directions, longitudinal and transversal, which are beneficial to the weld as it improves the resistance to crack propagation; therefore, it helps to avoid fatigue failure [24]. For the other weld conditions (600 rpm with 100 mm/min and 1500 rpm with 300 mm/min) the residual stresses in the transversal direction are tensile of approximately 20 MPa. However, taking into account that the measurement technique of residual stresses by X-ray diffraction has a measurement uncertainty of ± 15 MPa, the residual stresses with magnitudes lower than 20 MPa can be disregarded; therefore, the stir zone of the weld produced by a smooth pin is considered a stress-free material for all the evaluated cases.
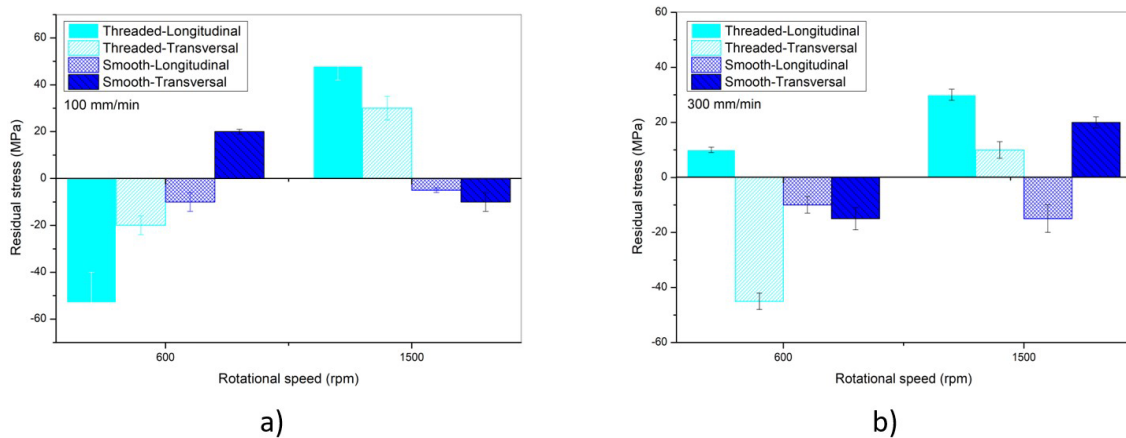
Figure 7. Residual stresses only for the rotational speeds: 600 and 1500 rpm, at welding speeds: (a) 100 and (b) 300 mm/min.

The residual stresses for the threaded pin show that, the residual compressive stresses are presented for lower rotational speeds. Only the weld condition of 600 rpm with 100 mm/min presented residual stresses fully compressive. The welds obtained from 600 rpm and 300 mm/min presented a compressive stress of 45 MPa in the transversal direction and a small tensile stress of 13 MPa in the longitudinal direction that can be disregarded as it presents a magnitude lower than 15 MPa. For the welds conducted with 1500 rpm, at 100 and 300 mm/min, the residual stresses are entirely tensile. In a numerical and experimental study, Buffa et al. [23] found that the tensile residual stress in FSW increases with the increase of the rotational speed. In general, the smooth pin produced a smaller range for the residual stresses when compared to the threaded pin. This can be related to variations in the flow of the material and heat input into the process produced by the different tool pin profiles [31].

Table 7 presents the analysis of variance for the residual stresses in the longitudinal (L) and transversal (T) directions. The results show that, the residual stress in the longitudinal direction is mainly influenced by the rotational speed, followed by the pin shape, and finally by the welding speed. There are interactions between the effects of these factors on the residual stress in longitudinal and transversal directions. However, the residual stress in the transversal direction is firstly influenced by the rotational speed, secondly by the welding speed, and finally by the pin shape.

Influence of Pin Shape Geometry on the Torque, Forces, and Residual Stresses in
Friction Stir Welding of 5052-H34 Aluminum Alloy

Quintana et al.

Even using the same pin and the same process conditions, the residual stresses can vary along the weld bead, if the heat input changes along the joint. However, considering the restrictions imposed by the transversal areas adjacent to the weld, the residual stresses also vary laterally [32]. As residual stresses are self-balancing, it is expected that they will vary in depth within the weld in order to maintain balance.

Table 7. Analysis of variance (ANOVA) for the residual stress in the longitudinal (L) and transversal (T) directions.

Source	Sum square		Dof	Mean square		F		p-level	
	L	T	L-T	L	T	L	T	L	T
ω	5490.4	4565.04	1	5490.37	4565.04	168.29	363.99	0	1.97773×10^{-12}
v_w	459.4	950.04	1	459.37	950.04	14.08	75.75	0.0017	1.82734×10^{-7}
P_s	2109.4	590.04	1	2109.37	590.04	64.66	47.05	0	3.84104×10^{-6}
$\omega * v_w$	3105.4	1855.04	1	3105.37	1855.04	95.18	147.91	0	1.69409×10^{-9}
$\omega * P_s$	5490.4	3725.04	1	5490.37	3725.04	168.29	297.01	0	9.36825×10^{-12}
$v_w * P_s$	1134.4	590.04	1	1134.37	590.04	34.77	47.05	0	3.84104×10^{-6}
$\omega * v_w * P_s$	1890.4	1365.04	1	1890.37	1365.04	57.94	108.84	0	1.51884×10^{-8}
Error	522	200.67	16	32.63	12.54				
Total	20201.6	13840.96	23						

Some correlations between the residual stresses and the torque and forces are found in the experimental analysis. During the welding phase, a relation between the residual stresses and the torque and the axial force is observed. For lower rotational speeds (600 rpm) the threaded pin presents mainly residual compressive stresses (Figure 7). In these cases, the torque (Figure 4b) and the axial force (Figure 5b) in the welding phase are equal or lower for the threaded pin. While for higher rotational speeds (1500 rpm), the threaded pin presents residual stresses fully tensile (Figure 7) and the torque (Figure 4) and axial force (Figure 5) are higher than the values observed for the smooth pin.

Additionally, as the welding force acts in the longitudinal direction, the results show a relation between the residual stress in this direction and the welding force, for lower rotational speeds. For 600 rpm and 100 mm/min, the welding force (Figure 6a) is lower for the threaded pin which presents a residual stress more compressive than the smooth pin in the longitudinal direction (Figure 7). While for 600 rpm and 300 mm/min, the welding force (Figure 6b) is higher for the threaded pin which, in this case, presents a residual tensile stress in the longitudinal direction (Figure 7). For high rotational speeds, an equivalent relation between the welding force and the residual stress is not observed.

4. Conclusions

In this paper, the influence of the tool pin shape on the axial, welding, and transverse forces, the torque, and the residual stresses were analyzed for several combinations of rotational and welding speeds and pin shapes (threaded and smooth). From the experimental analysis, the following conclusions can be drawn:

- The maximum torque and axial force values, which happen in the plunging phase, are higher for the threaded pin for all welding conditions. While in the welding phase, the behavior of the torque and axial force in relation to the pin profiles depends on the welding conditions. In general, the threaded pin diminishes the welding force and increases the transverse force when compared to the smooth pin;

- The residual stresses in the stir zone present higher magnitudes for the threaded pin than the smooth pin. For higher rotational speeds, the residual stresses for the threaded pin are fully tensile. Additionally, the welding force is related to the residual stresses in the longitudinal direction, for low rotational speeds;

- In general, the effect of the threaded pin on the torque, forces, and residual stresses depends on the rotational speeds; therefore, the influence of the threaded pin on the material is probably affected by the increase of the heat input into the process;

- According to the ANOVA, there is an interaction between the effects of the rotational speed and pin shape factors on the torque and on the axial force, during the plunging phase. On the other hand, during the welding phase, the torque, forces, and residual stresses are influenced by the interaction of the three factors: rotational and welding speeds and the pin shape. These interactions suggested that the influence of the concerned factors on the variables must be analyzed together.

Influence of Pin Shape Geometry on the Torque, Forces, and Residual Stresses in
Friction Stir Welding of 5052-H34 Aluminum Alloy

Quintana et al.

References

[1] Çam G, Mistikoglu SJ. Recent developments in friction stir welding of al-alloys. Journal of Materials Engineering and Performance. 2014;23(6):1936-1953. http://dx.doi.org/10.1007/s11665-014-0968-x.

[2] Gangwar K, Ramulu M. Friction stir welding of titanium alloys: a review. Materials and Design. 2018;141:230-255. http://dx.doi.org/10.1016/j.matdes.2017.12.033.

[3] Huang Y, Meng X, Xie Y, Wan L, Lv Z, Cao J, et al. Friction stir welding/processing of polymers and polymer matrix composites. Composites. 2018;A105:235-257. http://dx.doi.org/10.1016/j.compositesa.2017.12.005.

[4] Bist A, Saini JS, Sharma B. A review of tool wear prediction during friction stir welding of aluminum matrix composite. Transactions of Nonferrous Metals Society of China. 2016;26(8):2003-2018. http://dx.doi.org/10.1016/S1003-6326(16)64318-2.

[5] Bilgin MB, Meran C, Canyurt OE. Optimization of strength of friction stir welded joints for AISI 430 ferritic stainless steels by genetic algorithm. International Journal of Advanced Manufacturing Technology. 2015;77(9-12):2221-2233. http://dx.doi.org/10.1007/s00170-014-6590-0.

[6] Gao S, Zhao H, Zhang R, Ma C, Zhou L, Chen G, et al. Microstructure evolution of friction stir processed 2507 duplex stainless steel. Welding in the World. 2021;65(12):2349-2358. http://dx.doi.org/10.1007/s40194-021-01175-3.

[7] Landell RM, Lessa CR, Bergmann L, Santos JF, Kwietniewski CE, Klusemann B. Investigation of friction stir welding process applied to ASTM 572 steel plate cladded with Inconel®625. Welding in the World. 2021;65(3):393-403. http://dx.doi.org/10.1007/s40194-020-01007-w.

[8] Shah LH, Othman NH, Gerlich A. Review of research progress on aluminum-magnesium dissimilar friction stir welding. Science and Technology of Welding and Joining. 2017;23(3):256-270. http://dx.doi.org/10.1080/13621718.2017.1370193.

[9] Shrivastava A, Zinn M, Duffie NA, Ferrier NJ, Smith CB, Pfefferkorn FE. Force measurement-based discontinuity detection during friction stir welding. Journal of Manufacturing Processes. 2017;26:113-121. http://dx.doi.org/10.1016/j.jmapro.2017.01.007.

[10] Jain R, Pal SK, Singh SB. A study on the variation of forces and temperature in a friction stir welding process: a finite element approach. Journal of Manufacturing Processes. 2016;23:278-286. http://dx.doi.org/10.1016/j.jmapro.2016.04.008.

[11] Quintana KJ, Silveira JL. Analysis for the forces in FSW for aluminum alloy considering tool geometry and process. Journal of the Brazilian Society of Mechanical Sciences and Engineering, Brazil. 2018;40(4):229-240. http://dx.doi.org/10.1007/s40430-018-1162-0.

[12] Dialami N, Cervera M, Chiumenti M, De Saracibar C. A fast and accurate two-stage strategy to evaluate the effect of the pin tool profile on metal flow, torque and forces in friction stir welding. International Journal of Mechanical Sciences. 2017;122:215-227. http://dx.doi.org/10.1016/j.ijmecsci.2016.12.016.

[13] Quintana KJ, Silveira JL. Analysis of torque in friction stir welding of aluminum alloy 5052 by inverse problem method. ASME Journal of Manufacturing Science and Engineering. 2017;139(4):041017. http://dx.doi.org/10.1115/1.4035719.

[14] Cui S, Chen ZW, Robson JD. A model relating tool torque and its associated power and specific energy to rotation and forward speeds during friction stir welding/processing. International Journal of Machine Tools and Manufacture. 2010;50(12):1023-1030. http://dx.doi.org/10.1016/j.ijmachtools.2010.09.005.

[15] Rose AR, Manisekar K, Balasubramanian V. Effect of plunging force on microstructure and tensile properties of friction stir welded AZ61A magnesium alloy. Transactions of Nonferrous Metals Society of China. 2011;21(5):974-984. http://dx.doi.org/10.1016/S1003-6326(11)60809-1.

[16] Zhao S, Bi Q, Wang Y. An axial force controller with delay compensation for the friction stir welding process. International Journal of Advanced Manufacturing Technology. 2016;85(9-12):2623-2638. http://dx.doi.org/10.1007/s00170-015-8096-9.

[17] Mehta M, Chatterjee K, De A. Monitoring torque and transverse force in friction stir welding from input electrical signatures of driving motors. Science and Technology of Welding and Joining. 2013;18(3):191-197. http://dx.doi.org/10.1179/1362171812Y.0000000084.

[18] Su H, Wu CS, Pittner A, Rethmeier M. Simultaneous measurement of tool torque, transverse force and plunging force in friction stir welding. Journal of Manufacturing Processes. 2013;15(4):495-500. http://dx.doi.org/10.1016/j.jmapro.2013.09.001.

[19] Mishra RS, Ma ZY. Friction stir welding and processing. Materials Science and Engineering R Reports. 2005;50(1-2):1-78. http://dx.doi.org/10.1016/j.mser.2005.07.001.

[20] Rao CV, Reddy GM, Rao KS. Influence of tool pin profile on microstructure and corrosion behavior of AA2219 Al-Cu alloy friction stir weld nuggets. Defence Technology. 2015;11(3):197-208. http://dx.doi.org/10.1016/j.dt.2015.04.004.

[21] Nandan R, Debroy T, Bhadeshia HKDH. Recent advances in friction-stir welding-process, weldment structure and properties. Progress in Materials Science. 2008;53(6):980-1023. http://dx.doi.org/10.1016/j.pmatsci.2008.05.001.

[22] Xu Y, Bao R. Residual stress determination in friction stir butt welded joints using a digital image correlation-aided slitting technique. Chinese Journal of Aeronautics. 2017;30(3):1258-1269. http://dx.doi.org/10.1016/j.cja.2016.11.003.

Influence of Pin Shape Geometry on the Torque, Forces, and Residual Stresses in
Friction Stir Welding of 5052-H34 Aluminum Alloy

Quintana et al.

[23] Buffa G, Fratini L, Marannano G, Pasta A. Effect of the mutual position between weld seam and reinforcement on the residual stress distribution in Friction Stir Welding of AA6082 skin and stringer structures. Thin-Walled Structures. 2016;103:62-71. http://dx.doi.org/10.1016/j.tws.2016.02.003.

[24] Sousa LA, Souza LFG, Cindra FM. Characterization of mechanical properties and residual stress in API 5L X80 steel welded joints. Journal of Materials Engineering and Performance. 2018;27(1):124-137. http://dx.doi.org/10.1007/s11665-017-3090-z.

[25] Aval HJ. Microstructure and residual stress distributions in friction stir welding of dissimilar aluminum alloys. Materials and Design. 2015;87:405-413. http://dx.doi.org/10.1016/j.matdes.2015.08.050.

[26] Zapata J, Toro M, López D. Residual stresses in friction stir dissimilar welding of aluminum alloys. Journal of Materials Processing Technology. 2016;229:121-127. http://dx.doi.org/10.1016/j.jmatprotec.2015.08.026.

[27] Kumar R, Singh K, Pandey S. Process forces and heat input as function of process parameters in AA5083 friction stir welds. Transactions of Nonferrous Metals Society of China. 2012;22(2):288-298. http://dx.doi.org/10.1016/S1003-6326(11)61173-4.

[28] Quintana KJ, Silveira JL. Mechanistic models and experimental analysis for the torque in FSW considering the tool geometry and the process velocities. Journal of Manufacturing Processes. 2017;30:406-417. http://dx.doi.org/10.1016/j.jmapro.2017.09.031.

[29] Withers PJ, Bhadeshia HKDH. Residual stress. Part 1 – measurement techniques. Materials Science and Technology. 2001;17(4):355-365. http://dx.doi.org/10.1179/026708301101509980.

[30] Jain R, Pal SK, Singh SB. Finite element simulation of pin shape influence on material flow, forces in friction stir welding. International Journal of Advanced Manufacturing Technology. 2018;94(5-8):1781-1797. http://dx.doi.org/10.1007/s00170-017-0215-3.

[31] Reza-E-Rabby M, Tang W, Reynolds AP. Effect of tool pin features on process response variables during friction stir welding of dissimilar aluminum alloys. Science and Technology of Welding and Joining. 2015;20(5):425-432. http://dx.doi.org/10.1179/1362171815Y.0000000036.

[32] He W, Liu J, Hu W, Wang G, Chen W. Controlling residual stress and distortion of friction stir welding joint by external stationary shoulder. High-Temperature Materials and Processes. 2019;38(2019):662-671. http://dx.doi.org/10.1515/htmp-2019-0005.